Carrier-Transport, Photoluminescence, and Electroluminescence Properties Comparison of a Series of Terbium Complexes with Different Structures

Hao Xin,[†] Mei Shi,[‡] Xiao Mei Zhang,[§] Fu You Li,[‡] Zu Qiang Bian,[†] K. Ibrahim,[||] Feng Qin Liu,[||] and Chun Hui Huang*,[†,‡]

State Key Laboratory of Rare Earth Materials Chemistry and Applications, Peking University, Beijing, 100871, P. R. China; Institute of Advanced Materials and Technology, Fudan University, Shanghai, 200433, P.R. China; Department of Chemical Biology, College of Chemistry and Molecular Engineering, Peking University, Beijing, 100871, P. R. China; and Photoemission Spectroscopy Station, Institute of High Energy Physics, Chinese Academy of Sciences, Beijing 100039, P. R. China

Received June 3, 2003. Revised Manuscript Received July 9, 2003

A series of terbium complexes with different structures revealed different carrier-transport and photophysical properties. Complex A [tris(1-phenyl-3-methyl-4-isobutyl-5-pyrazolone)-bis(triphenyl phosphine oxide), $Tb(PMIP)_3(TPPO)_2$] had overly strong electron-transport properties, complex B [$Tb(PMIP)_3(EtOH)(H_2O)$] mainly revealed hole-transport properties, and complex C [tris(1-phenyl-3-methyl-4-(2-ethylbutyryl)-5-pyrazolone) triphenyl phosphine oxide, $Tb(eb\text{-}PMP)_3(TPPO)$] showed both electron- and hole-transport properties. Their PL intensity ratio was A−B−C = 2.6:1:1.2. The eletroluminescence (EL) performances (brightness and peak power efficiency) achieved from complexes A, B, and C were 9600 cd/m^2 and 5.21 lm/W, 2800 cd/m^2 and 2.61 lm/W, and 12000 cd/m^2 and 11.3 lm/W, from device configurations of ITO/TPD−B−A−AlQ−$Mg_{0.9}Ag_{0.1}$−Ag (20:20:50:30:200:80 nm), ITO/TPD−B−BCP−AlQ−$Mg_{0.9}Ag_{0.1}$)−Ag (40:30:20:20:200:80 nm), and ITO/NPB−C−BCP−AlQ−$Mg_{0.9}$-$Ag_{0.1}$−Ag (10:50:20:40:200:80 nm), respectively. Results indicated that for a given terbium complex, balanced carrier injection and a well-confined recombination zone are crucial to obtaining maximum EL performance. More important, if this premise is satisfied, for different complexes, the higher the PL quantum yield the complex shows, the greatly improved the EL performance will be.

Introduction

Although numerous investigations on organic light-emitting diodes (OLEDs) using organic dyes and polymers are reported, lanthanide complexes are still of great interest [1−11] because they exhibit extremely sharp emission bands due to their 4f electrons which are responsible for their properties; furthermore, internal quantum efficiencies are not a limitation (up to 100%, theoretically) because both the singlet and triplet are involved in the luminescence process.[12] However, lanthanide complexes have not shown satisfying electroluminescence (EL) performance: the best record was 2000 cd/m^2 and 2.6 lm/W reported by V. Christou[9] after our reported[7] performance of 960 cd/m^2 and 0.51 lm/W from terbium complex $Tb(PMIP)_3(TPPO)_2$ (A) (chemical structure shown in Figure 1, where PMIP and TPPO stand for 1-phenyl-3-methyl-4-isobutyryl-5-pyrazolone and triphenyl phosphine oxide, respectively). Experimental results revealed this complex had overly strong electron-transport properties, charge carriers mainly recombined in the hole-transport layer in devices using it as emitter, leading to poor EL performance. In contrast, complex $Tb(PMIP)_3(EtOH)(H_2O)$ (B), mainly showed hole-transport properties; based on this, by modifying the ligand, we synthesized a new terbium complex tris(1-phenyl-3-methyl-4-isobutyl-5-pyrazolone)-bis(triphenyl phosphine oxide) terbium [$Tb(eb\text{-}PMP)_3TPPO$, (C)] (Figure

* To whom correspondence should be addressed. E-mail: hch@chem.pku.edu.cn. Tel.: +86-(10) 62757156 Fax: +86-(10) 62757156.
[†] State Key Laboratory of Rare Earth Materials Chemistry and Applications.
[‡] Institute of Advanced Materials and Technology, Fudan University.
[§] Department of Chemical Biology, Peking University.
[||] Chinese Academy of Sciences.

(1) Kido, J.; Nagai, K.; Ohashi, Y. *Chem. Lett.* **1990**, 657.
(2) Kido, J.; Nagai, K.; Okamoto, Y. *J. Alloys Compd.* **1993**, *192*, 30.
(3) Kido, J.; Hayase, H.; Hongawa, K.; Nagai, K.; Okuyama, K. *Appl. Phys. Lett.* **1994**, *65*, 2124.
(4) Sano, T.; Fujita, M.; Fujii, T.; Hamada, Y. *Jpn. J. Appl. Phys.* **1995**, *34*, 1883.
(5) McGehee, M. D.; Bergstedt, T.; Zhang, C.; Saab, A. P.; O'Regan, M. B.; Bazan, G. C.; Srdanov, V. I.; Heeger, A. J. *Adv. Mater.* **1999**, *11*, 1340.
(6) Hu, W. P.; Matsumura, M.; Wang, M. Z.; Jin, L. P. *Appl. Phys. Lett.* **2000**, *77*, 4271.
(7) Gao, X. C.; Cao, H.; Huang, C. H.; Li, B. G.; Umitani, S. *Appl. Phys. Lett.* **1998**, *72*, 2217.
(8) Gao, X. C.; Cao, H.; Huang, C. H.; Umitani, S.; Chen, G. Q.; Jiang, P. *Synth. Met.* **1999,** *99*, 127.
(9) Capecchi, S.; Renault, O.; Moon, D.-G.; Halim, M.; Etchells, M.; Dobson, P. J.; Salata, O. V.; Christou, V. *Adv. Mater.* **2000**, *12*, 1591.
(10) Wang, J. F.; Wang, R. Y.; Yang, J.; Zheng, Z. P. *J. Am. Chem. Soc.* **2001**, *123*, 6179.
(11) Zheng, Y. X.; Liang, J. L.; Lin, Q.; Yu, Y. N.; Meng, Q. G.; Zhou, Y. H.; Wang, S. B.; Wang, H. A.; Zhang, H. J. *J. Mater. Chem.* **2001,** *11*, 2615.
(12) Kido, J.; Okamot, Y. *Chem. Rev.* **2002**, *102*, 2357.

10.1021/cm0344414 CCC: $25.00
Published on Web 08/21/2003

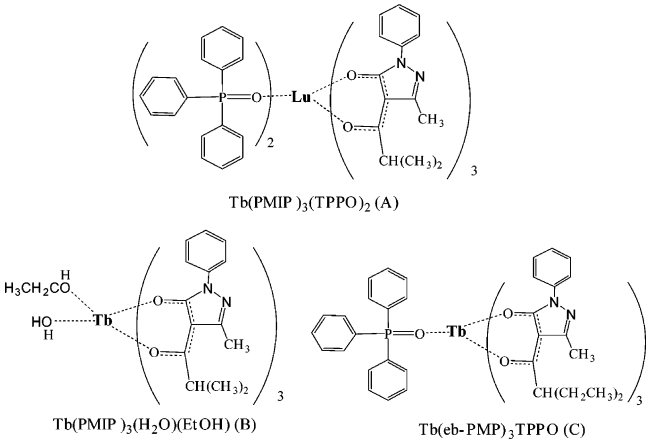

Figure 1. Chemical structures of the three complexes.

1) with one TPPO coordinated. Considering the coordinative number of lanthanide complexes is changeable, the goal in making this modification is to enlarge the steric hindrance of the β-diketonate and make a surrounding which has no room for two TPPOs to coordinate to the central Tb^{3+} ions. As expected, in this complex hole- and electron-transport were relatively balanced, and leading carriers were easily confined in the complex layer in a device with the configuration ITP/TPD−C−BCP−AlQ−$Mg_{0.9}Ag_{0.1}$ (10:50:20:40 nm) and remarkable EL performance was achieved.[13]

In this article, the charge carrier transport, PL, and EL properties of the three complexes are investigated and compared in detail.

Experimental Section

Materials. 1-Phenyl-3-methyl-4-isobutyryl-5-pyrazolone (PMIP) was synthesized in our laboratory.[8] The hole-transport material N, N′-diphenyl-N,N′-bis(3-methylphenyl)-1,1′-biphenyl-4,4′-diamine (TPD, 99%) was purchased from Aldrich, N,N′-diphenyl-N,N′-bis(1-naphthyl)-1,1′-diphenyl-4,4′-diamine (NPB) was kindly supplied by Technical Institute of Physics and Chemistry, Chinese Academy of Science as a gift, and hole-blocking material 2,9-dimethyl-4,7-diphenyl-1,10-phenyanthroline (BCP, 98%) was obtained from Acros; all were used as supplied. Tris(8-hydroxyquinolinato) alumimium (AlQ) was synthesized in our lab and sublimated two times before use. Indium tin oxide (ITO) glass substrate with a sheet resistance of 15 Ω/□ was kindly sent by China Southern Glass Holding Co. Ltd. as a gift.

Synthesis. *Synthesis of the Ligand eb-PMP.* 1-Phenyl-3-methyl-pyrazolone-5 (PMP) (7.5 g, 0.05 mol) and 150 mL of dried 1,4-dioxane were placed in a 250-mL flask with a magnetic stirrer and heated at 70 °C for 10 min. To the resulting yellow solution, calcium hydroxide (9 g, 0.18 mol) and barium hydroxide (1 g, 0.03 mol) in small portions were added, and then 2-ethylbutyryl chloride (8 mL, 0.058 mol) was added dropwise. The resulting mixture was heated to reflux for 24 h. The cloudy pinkish mixture was cooled to room temperature and poured into a stirred solution of ice-cold hydrochloric acid (350 mL of a 3 mol L^{-1} solution). The pink oil that precipitated was extracted by chloroform and washed extensively using deionized water and dried with anhydrous sodium sulfate. Then the oil product was purified by chromatograph on a silica gel column with $CHCl_3$/oil ether (20:1, v/v) as an eluent to get pale yellow oil with the yield of 40%. ^1H NMR (200 MHz, $CDCl_3$) (Figure 1), δ: 7.87 (2H); 7.44 (2H); 7.29 (2H); 2.85 (1H); 2.48 (3H); 1.79 (4H); 0.94 (6H).

Synthesis of the Complexes. Complexes A, B, and C were synthesized according to the method reported previously.[8]

$Tb(PMIP)_3(TPPO)_2$ (A): To a 50-mL ethanol solution containing 1 mmol $TbCl_3$, 3 mmol 1-phenyl-3-methyl-4-isobutyryl-5-pyrazolone (PMIP), and 2 mmol TPPO, 3 mL of 1.0 mol L^{-1} NaOH was added dropwise under stirring, and the solution was heated to refluxing for 5 h. The resulting solution was filtered and the colorless crystal was obtained after 2 days. It was purified by recrystallization from ethanol solution. Found (%): C, 64.70; H, 5.32; N, 5.75. Calcd. (%) for $C_{78}H_{75}N_6O_8P_2$-Tb: C, 64.68; H, 5.22; N, 5.80.

$Tb(PMIP)_3(EtOH)(H_2O)$(B): To a 50- mL ethanol solution containing 1 mmol $TbCl_3$ and 3 mmol 1-phenyl-3-methyl-4-isobutyryl-5-pyrazolone (PMIP), 3 mL of 1.0 mol L^{-1} NaOH was added dropwise under stirring, and the solution was heated to refluxing for 5 h. The resulting solution was filtered and the white powder was obtained. It was purified by recrystallization from ethanol solution. Found (%): C, 55.00; H, 5.54; N, 8.60. Calcd. (%) for $C_{44}H_{53}N_6O_8Tb$: C, 55.20; H, 5.54; N, 8.78.

$Tb(eb\text{-}PMP)_3TPPO$ (C): To a 50-mL ethanol solution containing 1 mmol $TbCl_3$, 3 mmol 1-phenyl-3-methyl-4-(2-ethylbutyryl)-5-pyrazolone (eb-PMP), and 2 mmol TPPO, 3 mL of 1.0 mol L^{-1} NaOH was added dropwise under stirring, and the solution was heated to refluxing for 24 h. The resulting solution was filtered and the colorless crystal was obtained after 2 days. It was purified by recrystallization from ethanol solution. Found (%): C, 63.44; H, 5.79; N, 6.70. Calcd. (%) for $C_{66}H_{72}N_6O_7PTb$: C, 63.14; H, 5.74; N, 6.70.

Preparation of EL Devices. Organic layers were sequentially deposited in one run by high vacuum (9×10^{-4}Pa) thermal evaporation onto a precleaned ITO glass substrate. A shadow mask with 5-mm diameter openings was used to define the cathode of a 200-nm thick layer of $Mg_{0.9}Ag_{0.1}$ alloy, with a 100-nm thick Ag cap. The thickness of the deposited layer and the evaporation speed of the individual materials were monitored in a vacuum with quartz crystal monitors. The deposition rates were maintained to be 0.1−0.3 nm s^{-1} for organic materials and 1.0−1.3 nm s^{-1} for $Mg_{0.9}$:$Ag_{0.1}$ alloy.

Apparatus. FT-IR spectra were taken on a Nicolet MAGNA-IR spectrometer. The photoluminescence and electroluminescence spectra were measured on a Hitachi F-4500 fluorescence spectrophotometer. UV−visible absorption spectra were recorded using a Shimadzu 3100 UV−Vis−NIR spectrophotometer. The current−voltage (I−V) and luminance−voltage (L−V) characteristics were measured with a computer-controlled Keithley 2400 Sourcemeter unit with a calibrated silicon diode. Synchrotron radiation photon-electron spectroscopy (SRPES) was measured on a photon-electron spectrometer (VSW Scientific Instruments, Ltd.) through synchrotron radiation under ultrahigh vacuum ($(3-4) \times 10^{-8}$Pa). Photon-electron spectrum was recorded under 32.7 eV synchrotron radiation light.

Results and Discussion

Characterization. TG analysis curves of complexes B and C are shown in Figure 2. It is clear that in the temperature range 80−130 °C complex B lost its weight by 6.8%, which is equal to the weight percent (6.7%) of water and ethanol molecules in it, while complex C was very stable at temperatures below 300 °C, and complex A revealed the same characteristic as complex C. The FT−IR spectrum of complex B (Figure 3) measured from its 80-nm thickness vacuum-evaporated film on Si slide did not show any peak at the range of 3200−3500 cm^{-1}, implying that there are no OH vibrations in the evaporated film, and further confirmed that complex B lost its coordinated small molecules during vacuum evaporation and so it is $Tb(PMIP)_3$ acting as emitting material in the corresponding fabricated devices.

(13) Xin, H.; Li, F. Y.; Shi, M.; Bian, Z. Q.; Huang, C. H. *J. Am. Chem. Soc.* **2003**, *125*, 7166.

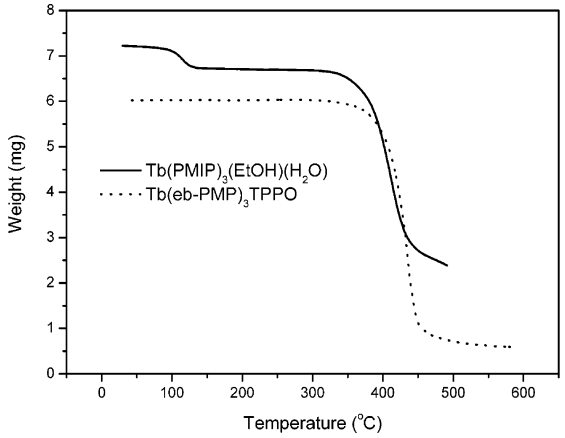

Figure 2. TG curves of complexes B and C.

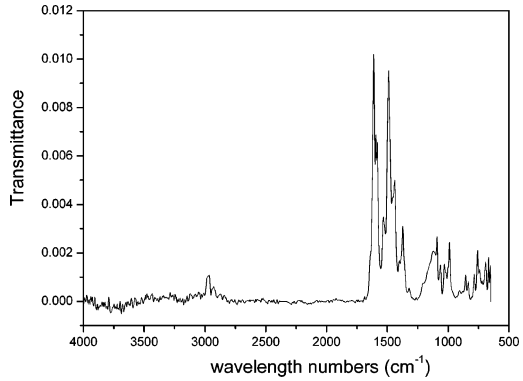

Figure 3. FT−IR spectrum of 60-nm film of complex B evaporated on Si slide.

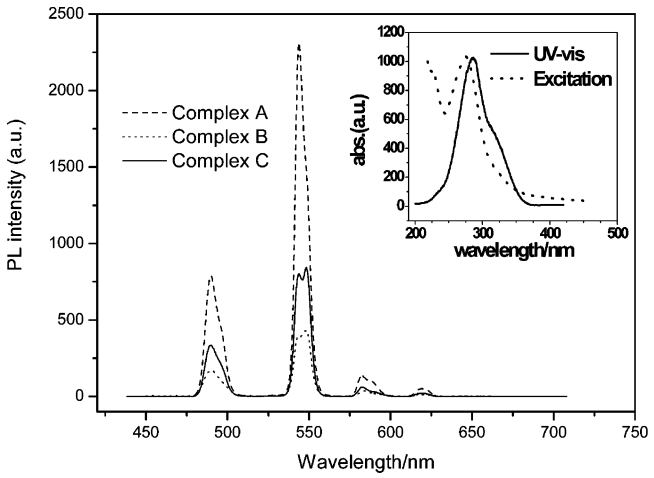

Figure 4. PL spectra of complexes A, B, and C (Inset: UV−vis and excitation spectra of complex B) at exciting wavelength 285 nm measured from their 80-nm vacuum evaporated films on quartz slides.

PL Properties. The PL spectra of the three complexes measured at the same time from their 80-nm vacuum-evaporated films on quartz slides are shown in Figure 4; inset shows the UV−vis absorbance and excitation spectra of complex B (the other two complexes had the same characteristics). The excitation spectrum overlaid absorbance wavelength range well, indicating the emission was originated from the energy absorbed by the ligands. However, their relative PL intensities were quite different from each other: complex A was the strongest, complex B was the weakest, and complex C was of medium intensity. The PL intensity (integral area) ratio of the three complexes was A−B−C = 2.6:1:1.2. As the difference of the complexes was that they had different numbers of neutral ligand TPPO, so we can conclude that the neutral ligand TPPO can strengthen terbium complex PL intensity. Another difference was that the main emission peaking at about 545 nm of complex B and C split into two peaks at 542 and 548 nm and their half-width became wider compared to that of complex A, which maybe caused by the different coordination environments of the central ions.

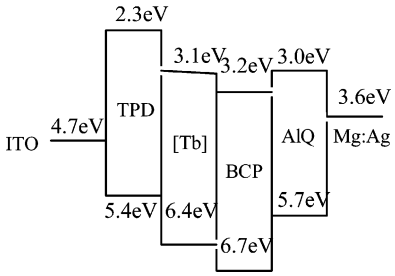

Figure 5. Energy diagram of the materials used.

HOMO and LUMO Energy Levels. From the photon-electron spectrum the first ionization energy (I_p, 6.40 eV) was obtained, the highest occupied molecule orbital (HOMO) energy level for each complex is equal to its I_p value. The lowest unoccupied molecular orbital (LUMO) energy of the complex is estimated on the basis of its HOMO level and the energy gap between HOMO and LUMO, which can be obtained by referring to the absorption spectrum (absorption edge, 3.35 eV) of the complex, thus, the LUMO value (3.05 eV) can be derived. The three complexes had the same energy levels.

EL Properties. *Single-Layer Devices.* The highest brightness obtained from the single-layer devices A1, B1, and C1, ITO/Tb-complex(80 nm)/$Mg_{0.9}Ag_{0.1}$(200 nm) /Ag(80 nm), respectively, using complexes A, B, and C as emitters, were 12, 8.3, and 46 cd/m^2, respectively, and all the three devices showed the same turn-on voltage of 11 V.

Three-Layer Devices. By introducing TPD and AlQ as hole- and electron-transport materials, devices A2, B2, and C2, having the same configuration of ITO/TPD−Tb-complex−AlQ−$Mg_{0.9}Ag_{0.1}$−Ag (20:50:30:200:80 nm), respectively, using complexes A, B, and C as emitter, were fabricated at the same condition. Compared to the single-layer device, the turn-on voltage of the three devices decreased to 4 V, attributed to the step injection of the holes due to the introduction of TPD (energy level diagram shown in Figure 5). The EL spectra (shown in Figure 6) revealed that for device A2, the emission was mainly from TPD with a small amount from terbium complex, and no emission from AlQ was detected, indicating complex A has very good electron-transport properties. For device B2, however, the main emission was from AlQ peaking at 520 nm, and no emission from TPD was detected, indicating that complex B mainly showed hole-transport properties. In device C2, the primary emission was from terbium complex, with a small part from TPD and AlQ as well, revealing electron and hole transport were relatively balanced in this complex. The highest brightness and power efficiencies achieved from the three devices were 2100 cd/m^2 at 13 V (0.18 A/cm^2) and 1.49 lm/W at 7 V (0.028 A/cm^2, 95

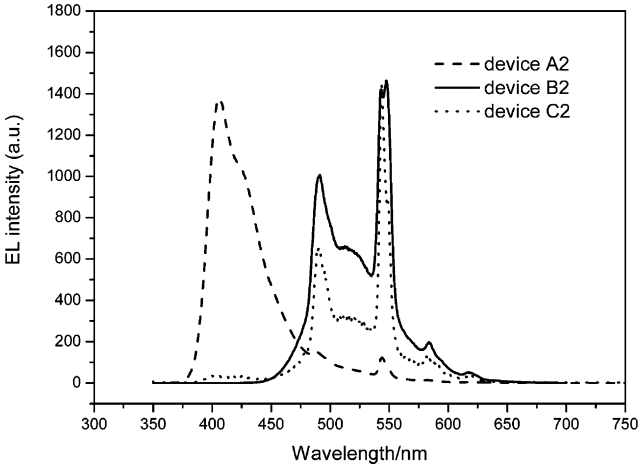

Figure 6. EL spectra of devices A2, B2, and C2 with the same configuration of TPD−Tb-complex−BCP−AlQ (20:50:20:30) at applied voltage 10 V.

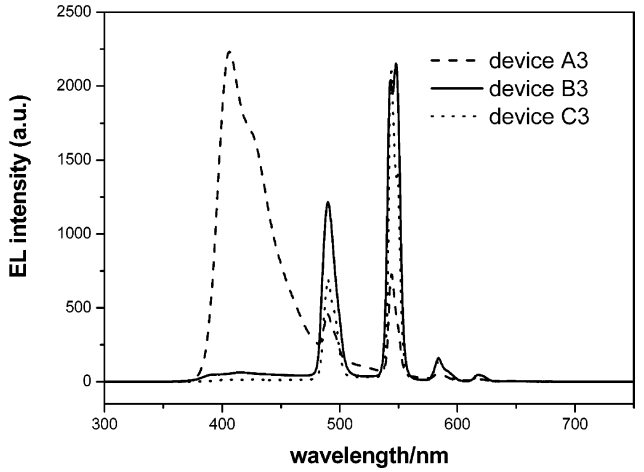

Figure 7. EL spectra of devices A3, B3, and C3 with the same configuration of ITO/TPD−Tb-complex−BCP−AlQ−$Mg_{0.9}Ag_{0.1}$−Ag (20:50:20:30:200:80 nm) at applied voltage 10 V.

cd/m^2) for device A2; 18 500 cd/m^2 at 21 V (0.61 A/cm^2) and 1.11 lm/W at 13 V (0.020 A/cm^2, 910 cd/m^2) for device B2; and 20 000 cd/m^2 at 20 V (0.95 A/cm^2) and 3.24 lm/W at 10 V (0.004 A/cm^2, 385 cd/m^2) for device C2, respectively. Although device C2 gave brightness similar to that of device B2, the power efficiency was much higher than that from the latter. This is because in device C2 the emission was mainly from terbium complex, which can utilize its triplet energy and its maximum internal quantum efficiency (100%), was much higher than that from AlQ (25%) in device B2.

Four-Layer Devices. After inserting hole-blocking material BCP between terbium complex and AlQ, devices A3 and C3 [having the same configuration of ITO/TPD−Tb-complex−BCP−AlQ−$Mg_{0.9}$–$Ag_{0.1}$−Ag (20:50:20:30:200:80 nm)] and device B3 [with the configuration of ITO/TPD−Tb-complex−BCP−AlQ−$Mg_{0.9}$-$Ag_{0.1}$−Ag (20:60:20:10:200:80 nm)] were made. Their EL spectra are shown in Figure 7. Devices B3 and C3 both gave the emission characteristic of central terbium ion, indicating that the carrier recombination zone was well confined in the complex layer and their performance was enhanced to 2640 cd/m^2 at 16 V (0.23 A/cm^2), 0.83 lm/W at 10 V (0.005 A/cm^2, 125 cd/m^2), and 8800 cd/m^2 at 18 V (0.53 A/cm^2), 9.4 lm/W at 7 V (0.0004 A/cm^2, 87 cd/

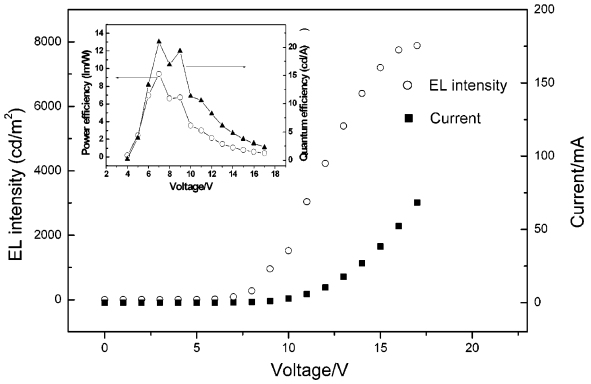

Figure 8. Current−voltage (■), luminance−voltage (○), and external quantum and power-efficiency (inset) curves of device C3.

m^2). For device A3, the primary emission still came from TPD although the proportion originating from terbium complex increased a little compared to that of device A2 and the performance was enhanced to 3100 cd/m^2 at 14 V (0.20 A/cm^2) and 3.62 lm/W at 6 V (0.00051 A/cm^2, 35.4 cd/m^2).

Current−voltage (I−V) and luminance-voltage (L−V) curves of device C3 are shown in Figure 8; the inset provides its power and quantum efficiency−voltage curves. Although the highest luminance was much lower than that from device C2, the peak power efficiency was enhanced nearly three times and it was still greater than 2.1 lm/W at brightness higher than 4300 cd/m^2, benefited from the special EL mechanism of lanthanide complexes mentioned above. The external quantum efficiency of device C3 was 21 cd/A.

By thickening the TPD and AlQ layers to strengthen hole and electron injection while keeping the total thickness unchanged, device B4 ITO/TPD−B−BCP−AlQ−$Mg_{0.9}Ag_{0.1}$−Ag (40:30:20:20:200:80 nm) achieved a performance of 2800 cd/m^2 at 12 V (0.13 A/cm^2) and 2.6 lm/W at 6 V (0.0002 A/cm^2, 11 cd/m^2). At lower voltage, device B4 emitted light solely from complex C as device B3, however, a little emission from AlQ appeared at applied voltage higher than 10, caused by the good hole-transport properties of complex B.

When hole-transport material TPD was replaced by NPB in device C4 having the same configuration as device C3 [ITO/NPB−C−BCP−AlQ−$Mg_{0.9}Ag_{0.1}$−Ag (20:50:20:30:200:80 nm)], the power efficiency was enhanced to 14.0 lm/W at 6 V (0.00023 A/cm^2, 62 cd/m^2), and the external quantum efficiency reached 28 cd/A, benefited from the low HOMO energy level of NBP (5.2 eV) which made the hole injection more easier. A luminance as high as 18 000 cd/m^2 at an applied voltage of 18 V (1.0 A/cm^2) was obtained from this device; however, the emission of NPB increased as the applied voltage increased (Figure 9) and the color changed to blue at this voltage, but at the peak power efficiency of device C4, the light was pure green as the emission of NPB was negligible. Thinning NPB to 10 nm and thickening AlQ to 40 nm in device C5 [ITO/NPB−complexC−BCP−AlQ−$Mg_{0.9}Ag_{0.1}$−Ag (10:50:20:40:200:80 nm)], the emission of NPB greatly decreased and a peak performance of 12 000 cd/m^2 at 18 V (0.5 A/cm^2) and 11.3 lm/W at 7 V (0.0001 A/cm^2, 274 cd/m^2) was achieved.

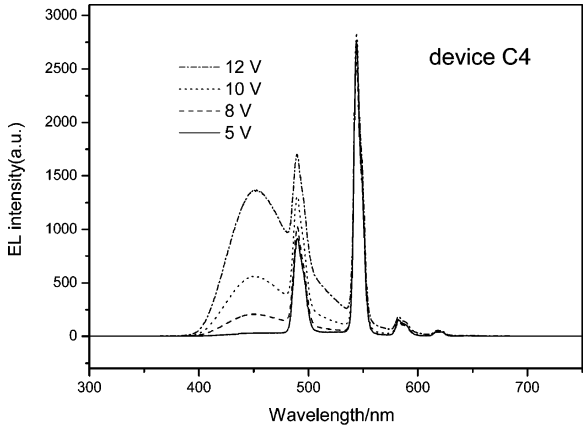

Figure 9. Normalized EL spectra of device C4 ITO/NPB−C−BCP−AlQ−$Mg_{0.9}Ag_{0.1}$−Ag (20:50:20:30:200:80 nm) at different applied voltages.

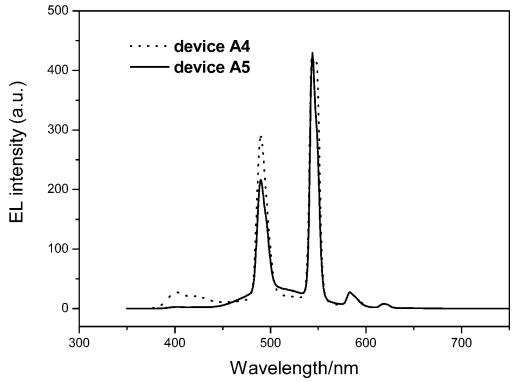

Figure 10. Normalized EL spectra of devices A4 and A5 at applied voltage 10 V. Device A4: ITO/TPD−B−A−AlQ−$Mg_{0.9}$-$Ag_{0.1}$−Ag (20:40:30:20:200:80 nm). Device A5: ITO/TPD−B−BCP−AlQ−$Mg_{0.9}Ag_{0.1}$−Ag (20:50:20:30:200:80 nm).

The above-mentioned devices A2 and A3 based on complex A mainly emitted light from TPD, indicating hole and electron were seriously unbalanced (hole was the minor) in the complex layer. Now, utilizing complex B to partly replace TPD as hole-transport layer, device A4 with the configuration ITO/TPD−B−A−AlQ−$Mg_{0.9}$-$Ag_{0.1}$−Ag (20:40:30:20:200:80 nm) was fabricated. The EL spectrum of device A4 (Figure 10) had the same characteristics as the PL of complex B with the main peak at 545 nm split into two peaks, indicating that in this device the exciton was mainly recombined in complex B, while complex A just acted as electron-transport material. The peak performance obtained from device A4 was 2400 cd/m^2 at 13 V (0.17 A/cm^2) and 0.77 lm/W at 9 V (0.016 A/cm^2) which was equal to the performance of device B3 ITO/TPD−B−BCP−AlQ−$Mg_{0.9}Ag_{0.1}$−Ag (20:50:20:30:200:80 nm). To make charge-carriers to recombine in complex A, by thinning AlQ layer to 30 nm to lower the electron injecting rate (because electron mobility was much lower than that of hole mobility), and thickening complex A layer to 50 nm to extend the recombination zone, device A5 with the configuration of ITO/TPD−B−A−AlQ−$Mg_{0.9}Ag_{0.1}$−Ag (20:20:50:30:200:80 nm) was made. The EL spectrum of this device (Figure 10) showed the PL characteristics of complex A, indicating the emission was primarily from complex A as expected. The output of device A5 improved to 9600 cd/m^2 at 15 V (0.15 A/cm^2) and 5.2 lm/W at 9 V (0.0016 A/cm^2), the external quantum efficiency was 16 cd/A; compared to device A4, this enhancement is due to the emission thatoriginated from complex A which showed much higher PL quantum yield than complex B. What should be noted is that in device A5 we have not introduced BCP to restrict holes from entering the electron-transport layer AlQ, so the emission from AlQ was detectable. The powder efficiency in device C3 was enhanced nearly 3 times (from 3.24 lm/W to 9.4 lm/W) after BCP was used, so it is reasonable expected the efficiency would greatly increase if more proper hole transport material was used to further balance carrier injection and BCP was introduced to completely confine the exciton in the emitting layer.

Table 1. Photoluminescence and Electroluminescence Properties of the Three Complexes[a]

complex	PL intensity	carrier-transport	luminance (cd/m^2)	efficiency (lm/W)
A	2.6	electron (overly strong)	9600[b]	5.2[b]
B	1	hole	2800	2.6
C	1.2	hole and electron	8800	9.4

[a] EL results were obtained from four-layer devices with TPD as hole-transport material. [b] Obtained from device A5, no BCP layer was used.

The three complexes with different numbers of neutral ligand TPPO showed quite different carrier-transport, PL, and EL properties (the results are summarized in Table 1). The PL intensity ratio was A−B−C = 2.6:1:1.2. Complex C with one TPPO showed both electron- and hole-transport properties, so carrier injection could be easily balanced, leading the recombination zone well confined in the emitting layer, and a satisfying performance (8800 cd/m^2 and 9.4 lm/W) was achieved. Although complex B with no TPPO mainly revealed hole-transport properties, experimental results indicated that after introducing hole-block layer BCP, exciton also could be well restricted in the complex layer. However, the EL performance of complex C is nearly 4 times higher than that of complex B (2800 cd/m^2 and 2.6 lm/W), the only explanation is that the two complexes have different PL quantum yields, although the PL intensity of complex C is only a little higher than that of complex B (1.2:1). Unlike complexes B and C, complex A with two TPPOs showed overly strong electron-transport properties, leading carrier injection was extremely unbalanced in the same structural device as B and C and we failed to get pure green light originated from complex A. This situation was changed by some extent by using complex B to enhance hole injection in device A5; an output of 9600 cd/m^2 and 5.2 lm/W was achieved from complex A. However, even in device A5, the exciton had not been well confined in complex A layer because no BCP was used; and the device could not be further optimized because of the limitation of our experimental condition—the maximum number of evaporation sources was six.

Conclusion

Neutral ligand TPPO seriously affects terbium complex PL quantum yield and carrier-transport properties in OLED. Experiments revealed that for a given terbium complex balanced carrier injection and well-confined recombination zone were crucial to its EL performance.

However, for different complexes, if this premise is satisfied, terbium complex EL performance is strongly dependent on its PL quantum yield in that a little increase of PL intensity will lead to remarkable EL improvement. Thus, to achieve an excellent performance from lanthanide complexes, we should devote our efforts to two aspects: device configuration optimization and material design. It is reasonable to expect that rare earth complexes can exhibit remarkable performance by utilizing more matching material to balance carrier injection and by designing more proper device structures to confine the exciton in the complex layer.

Acknowledgment. We thank the State Key Program of Fundamental Research on Rare Earth Functional Materials (G 1998061308), NHTRDP 863 Program (2002AA324080), and NNSFC (20221101) for the financial support.

CM0344414